

# Guided Vortex Bullets

Carlos F. Sánchez<sup>1,2</sup>, Ángel Paredes<sup>2</sup>, Humberto Michinel<sup>2</sup>, Boris A. Malomed<sup>3,4</sup>, and José R. Salgueiro<sup>2</sup>

<sup>1</sup>*Grupo de Investigación en Física (GIF), Universidad Politécnica Salesiana, Cuenca, 010105, Ecuador.*

<sup>2</sup>*Instituto de Física e Ciencias Aeroespaciais (IFCAE), Universidad de Vigo, 32004 Ourense, Spain.*

<sup>3</sup>*Department of Physical Electronics, School of Electrical Engineering,*

*Faculty of Engineering, Tel Aviv University, Tel Aviv 69978, Israel.*

<sup>4</sup>*Instituto de Alta Investigación, Universidad de Tarapacá, Casilla 7D, Arica, Chile.*

By means of the variational method and numerical simulations, we demonstrate the existence of stable 3D nonlinear modes, *viz.* vortex “bullets”, in the form of pulsed beams carrying orbital angular momentum, that can self-trap in a 2D waveguiding structure. Despite the attractive self-interaction, which is necessary for producing the bullets (bright solitons), and which readily leads to the collapse in the 3D setting as well as to spontaneous splitting of vortex modes, we find a critical value of the trapping depth securing the stabilization of the vortex bullets. We identify experimental conditions for the creation of these topological modes in the context of coherent optical and matter waves. Collisions between the bullets moving in the unconfined direction are found to be elastic. These findings contribute to the understanding of self-trapping in nonlinear multidimensional systems and suggest new possibilities for the stabilization and control of 3D topological solitons.

PACS numbers: 42.65.Tg, 05.45.Yv, 42.65.Jx

*Introduction.*— Three-dimensional (3D) solitons [1], commonly referred to as *wave/optical bullets* [2] and modeled by generalized nonlinear Schrödinger equations (NLSEs) [3], offer a fundamental testbed for studying the dynamics of many coherent physical systems, from optical communications [4] to Bose-Einstein condensates [5–7], and from plasma physics [8] to cosmic structures [9]. These types of 3D solitary waves exist as stationary states due to the balance between linear dispersive/diffractive effects and nonlinear self-focusing, but they are usually prone to the collapse (catastrophic self-compression). As well as the modulational instability [10], the collapse is driven by the self-focusing nature of the nonlinearity [11, 12]. In addition to the collapse-induced instability of the fundamental (structureless) bullets, ones with embedded vorticity (which is characterized by the corresponding topological charge) are vulnerable to spontaneous splitting.

In quantum-matter settings, such as Bose-Einstein condensates (BECs) in ultracold bosonic gases, the complex wavefunction  $\Psi$ , which obeys the Gross-Pitaevskii equation (GPE), represents the order parameter in the framework of the mean-field (MF) approximation [13]. The trap confining the ultracold gas is represented by the GPE term with potential  $V(\mathbf{r})$ , while the effect of inter-atomic collisions is reduced, by the MF approximation, to the cubic term in GPE. The coefficient in front of the latter term is proportional to the respective scattering length (positive or negative, for repulsive and attractive interactions respectively) [14]. In optics, the structure of a linearly polarized electromagnetic pulsed beam, propagating in a nonlinear graded-index waveguide, is confined in the transverse directions by a linear refractive-index distribution that plays the role of the trapping potential, while the optical Kerr effect gives rise to the cubic self-focusing or defocusing depending on its sign [12]. The two-dimensional transversal potential, if

it is strong enough, contributes to the stabilization of the spatial soliton bullets in the case when widths of the soliton and potential are similar. In fact, fundamental soliton bullets where already reported for parabolic [15] and periodic [16] potentials. Also, in a parabolic potential, similar solutions were described in Ref. [17] though for a system with the defocusing nonlinearity and normal dispersion.

As mentioned above, imparting the vorticity to nonlinear waves which is quantified by the topological charge [18, 19], gives rise to much richer dynamics at the cost of fueling more instability due to the growth of the splitting perturbations patterned along the azimuthal coordinate [20]. Therefore, the realization of such fascinating modes is a highly challenging problem with many ramifications [21, 22], and precise control over the input wave and the balance of competing linear and nonlinear effects are crucially important for achieving sustained stable propagation [23–25].

In this work, we present the first, to the best of our knowledge, prediction of the existence of stable 3D vortex bullets sustained and guided by a combination of a shallow 2D trapping potential and self-attractive cubic nonlinearity (2D lattice potentials can maintain stable 3D composite solitary modes, built as a set of four density peaks with the vorticity represented by phase shifts between them[26]). Our starting point is a (3+1)D NLSE with the temporal ( $t$ ) and spatial ( $\mathbf{r}$ ) coordinates, which governs the propagation of a coherent wave of amplitude  $\Psi(\mathbf{r}, t)$  in the system with the cubic self-focusing term. An axisymmetric trapping potential,  $V(x, y)$ , is defined in the plane transverse to the propagation axis  $z$ , along which the wave packet propagates freely. We adopt a Gaussian potential  $V(x, y)$ , which is a commonly used experimental tool in BEC and optics.

By means of a variational approximation (VA) we predict approximate eigenstates of the corresponding NLSE.

The VA solutions are then used as an input to numerically solve the reduced axisymmetric problem by means of a finite-differences scheme [27] and a globally convergent Newton method. Finally, we apply the Vakhitov-Kolokolov (VK) necessary-stability criterion [28], and verify the full stability by simulating the perturbed evolution with the help of the standard beam propagation method.

*The model.*- We start by considering the GPE with the attractive cubic term and a shallow Gaussian trapping potential with the axial symmetry,  $V(\rho) = -\gamma \exp(-\rho^2/2)$ , where  $(\rho, \varphi)$  are the polar coordinates in the  $(x, y)$  plane. The respective GPE takes the usual scaled form,

$$i \frac{\partial \Psi}{\partial t} + \nabla^2 \Psi - V(\rho) \Psi + |\Psi|^2 \Psi = 0, \quad (1)$$

where  $\nabla^2$  is the kinetic-energy operator acting on coordinates  $(x, y, z)$ . The only free parameter in Eq. (1), which cannot be fixed by rescaling, is the strength  $\gamma > 0$  of the trapping potential  $V(\rho)$ . The same equation governs the propagation of a linearly polarized laser pulse in a cylindrical gradient-index waveguide with the focusing Kerr nonlinearity and anomalous group-velocity dispersion. In the latter case,  $\gamma$  is proportional to the maximum value of the local increase of the refractive index,  $t$  is the propagation distance, and  $z$  is the temporal coordinate in the reference frame moving with the group velocity of the carrier wave. Equation (1) conserves the norm  $N = \int |\Psi|^2 d^3 \mathbf{r}$ , angular momentum  $M_z = -i \int \Psi^* \partial_\varphi \Psi d^3 \mathbf{r}$ , and the Hamiltonian:

$$H = \int \left[ |\vec{\nabla} \Psi|^2 - \frac{1}{2} |\Psi|^4 - \gamma e^{-\rho^2/2} |\Psi|^2 \right] d^3 \mathbf{r}. \quad (2)$$

We consider stationary localized states carrying integer vorticity (topological charge)  $\ell$  and real chemical potential  $-\beta$  (in optics,  $\beta$  is the propagation constant):

$$\Psi(x, y, z, t) = \psi(\rho, z) e^{i(\ell\varphi + \beta t)}, \quad (3)$$

for which the virial identity [16] can be derived from Eq. (1):

$$H = -\beta N + \frac{1}{2} \int |\psi|^4 d^3 \mathbf{r}. \quad (4)$$

*The variational approximation (VA).*- In this work we fix on fundamental vortex modes, with  $\ell = 1$ , which may be approximated by the real variational ansatz for  $\psi$ , with transverse and axial (longitudinal) widths parameters,  $R$  and  $\eta$ :

$$\psi_{\text{VA}} = \sqrt{\frac{N}{2\pi\eta R^2}} \frac{1}{\rho} \exp\left(-\frac{\rho^2}{2R^2}\right) \operatorname{sech}\left(\frac{z}{\eta}\right). \quad (5)$$

Minimizing  $H$  with respect to  $R$  and  $\eta$  for fixed  $N$ , a straightforward calculation produces the following VA results:

$$\eta = \frac{16\pi R^2}{N}, \quad N = \frac{16\pi\sqrt{3}R}{(R^2+2)^{\frac{3}{2}}} \sqrt{(R^2+2)^3 - 4\gamma R^4}, \quad (6)$$

the respective Hamiltonian per particle being

$$\frac{H}{N} = \frac{1}{R^2} - \frac{8\gamma}{(R^2+2)^3}, \quad (7)$$

and  $\beta$  is calculated from Eq. (4) by inserting the obtained variational wavefunction. Thus, for a given trapping-potential strength  $\gamma$ , the VA predicts the existence of a family of stationary states parameterized by the variational radius  $R$ , while the respective chemical potential can be obtained from Eq. (4). Analyzing the respective Hessian matrix of the derivatives, we find that the VA solutions correspond to a local minimum of the Hamiltonian (hence, they may be stable) if and only if  $dN/dR < 0$ . Consequently, the domain of *potentially stable* states can be found by requiring that  $N(R)$  [Eq. (6)] has an inflection point satisfying  $N'(R) = N''(R) = 0$ , which leads to  $\gamma = 8/3$ ,  $R = \sqrt{2}$ . On the other hand there is also a limit value of  $\gamma$  for which there exist solutions with  $N \rightarrow 0$  and nonzero values of  $R$  ( $\eta$  diverging as  $N \rightarrow 0$ ). This limit value of  $\gamma$  can be found by requiring that the expression under the square root in Eq. (6) and its derivative vanish simultaneously, which leads to  $\gamma = 27/8$  and  $R = 2$ .

In Fig. 1(a) we plot the VA-predicted dependences  $H(N)$  for different values of  $\gamma$ . As can be seen in the picture, the cust catastrophe is present for  $\gamma > 8/3$ . The respective dependences  $N(R)$  are plotted Fig. 1 (b).

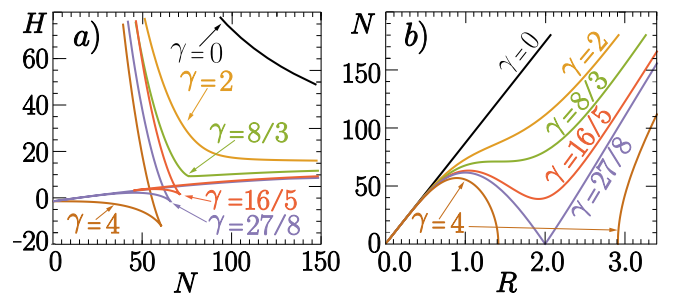


FIG. 1. a) Hamiltonian  $H$  vs. norm  $N$  for several values of the potential strength  $\gamma$ , as predicted by the VA. b) The VA-predicted dependences  $N$  on the transverse bullet's radius  $R$ , for the same set of values of  $\gamma$ .

*Numerical solutions.*- Once the VA solution has been found it is necessary to compare it with a numerical counterpart. Stationary states are solutions of the following eigenvalue problem for the real amplitude, produced by substitution  $\psi(\rho, z) = \rho^{-1/2} u(\rho, z)$ :

$$\frac{\partial^2 u}{\partial z^2} + \frac{\partial^2 u}{\partial \rho^2} - \frac{(\ell^2 - 1/4)}{\rho^2} u + \left[ \frac{u^2}{\rho} - V(\rho) - \beta \right] u = 0. \quad (8)$$

Equation (8) was solved by means of a finite-differences scheme [27], with the resulting nonlinear algebraic problem solved iteratively using a globally convergent Newton method. This technique is suitable, as the solutions have to meet the boundary condition  $\psi(0) = 0$  and thus  $u(0) = 0$ , yielding a regular behavior at  $\rho \rightarrow 0$ , in spite of the diverging factor  $\rho^{-1/2}$  in the above-mentioned substitution.

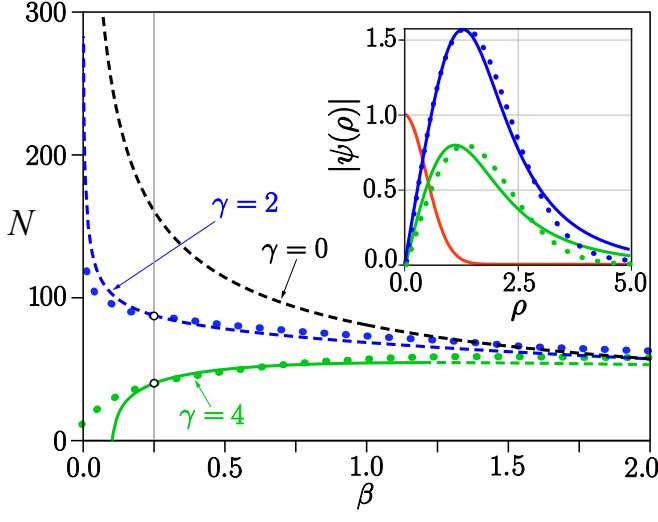


FIG. 2. Norm  $N$  of the numerically found stationary vortex solutions vs. the propagation constant  $\beta$  for different values of the waveguide strength parameter  $\gamma$ . Dashed and continuous lines indicate VK-unstable and VK-stable families respectively. The black (dashed) curve displays, for comparison, the family of unstable free-space solutions with  $\gamma = 0$ . Dotted lines represent the solutions obtained with the variational method. The inset shows numerical (solid) and variational (dotted) radial shapes of the solutions for  $\beta = 0.25$  [designated by the vertical gray line in the main plot and with the colors corresponding to those of the  $N(\beta)$  curves], along with the Gaussian trapping profile  $-V/\gamma$  (red curve).

Dependences  $N(\beta)$ , found numerically for  $\gamma = 0$  (free space),  $\gamma = 2$  and  $\gamma = 4$  are displayed, along with their VA-predicted counterparts in Fig. 2. Naturally, the deeper the trap is, the fewer particles are necessary to induce nonlinear self-trapping. Therefore, the values of  $N$  are lower for stronger potentials with higher values of  $\gamma$ . The free-space solitons, obtained for  $\gamma = 0$ , are definitely unstable, being included here for comparison. The continuous green ( $\gamma = 4$ ) and dashed blue ( $\gamma = 2$ ) curves represent, respectively, the solution families which are expected to be stable and unstable, according to the Vakhitov-Kolokolov (VK) stability criterion,  $dN/d\beta > 0$ , [1, 3, 12, 28]. The inset in Fig. 2 displays the Gaussian potential (the red curve) and stationary-solution profiles

for  $\beta = 0.25$ , designated by the vertical gray line in the main plot.

The blue  $N(\beta)$  curve in Fig. 2, which corresponds to a very shallow potential with  $\gamma = 2$ , is qualitatively similar to the free-space one for  $\gamma = 0$ . The increase of the trapping depth to  $\gamma > 4$  (the green curve) dramatically changes the situation, generating a cutoff value of the propagation constant,  $\beta_{\min} \approx 0.104$ , that correspond to the linear eigenstate ( $N = 0$ ) confined by the trapping potential in the  $(x, y)$  plane. Another notable consequence of making the trap stronger is that the green  $N(\beta)$  curve attains a (very flat) maximum around  $\beta = 1.24$ , beyond which the family is definitely VK-unstable, exhibiting  $dN/d\beta < 0$ .

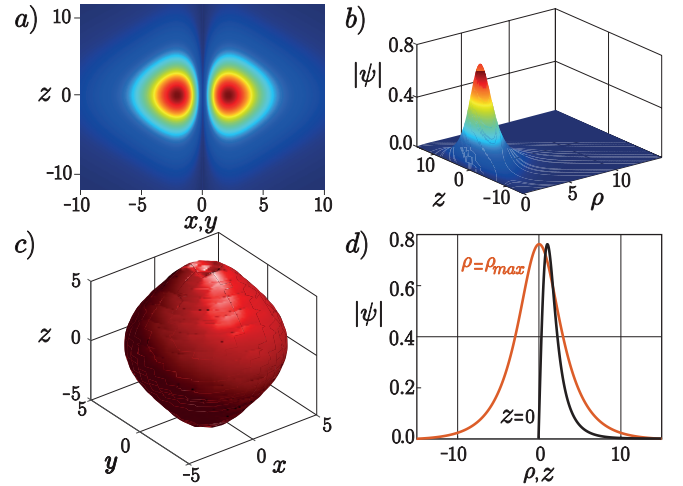


FIG. 3. A characteristic *stable* numerical solution of Eq. (8), with  $\gamma = 4$ ,  $\beta = 0.25$  and  $\ell = 1$ . Displayed are contour and mesh views of  $|\psi|$ , in a) and b), respectively. Panel c) shows the 3D isosurface, and d) plots the radial and axial (longitudinal) profiles of  $|\psi|$  at  $z = 0$  and  $\rho = \rho_{\max}$  (at  $\rho$  realizing the maximum of  $|\psi|$ ).

A characteristic example of the stationary vortex state is presented in Fig. 3, for  $\gamma = 4$  and  $\beta = 0.25$ , displaying the contour and mesh views in a) and b) respectively, of  $|\psi(x, y, z)|$  in plane  $(\rho, z)$ , along with the 3D isosurface view in c) and the cross-section profiles in d) at  $z = 0$  and  $\rho = \rho_{\max}$  (the value of  $\rho$  at which  $|\psi|$  attains its maximum). This solution is a stable one as shown below.

*The stability.* Because the VK criterion is only necessary but not sufficient for the full stability (particularly it cannot detect the plausible splitting instability of vortex solitons[1, 22]), final conclusions about the stability of stationary states satisfying the VK criterion were made by means of direct simulations of their perturbed propagation. The initial condition determines the topology of the emerging state provided that it is a stable one. This fact is important because it suggests that nontrivial vortex states may be experimentally created by means of choosing the appropriate input.

First, it was corroborated that all solution families

which do not satisfy the VK criterion are indeed unstable, such as those in Fig. 2 corresponding to  $\gamma = 0$  and  $\gamma = 2$ , as well as to  $\gamma = 4$  and  $\beta > 1.24$ . Characteristic examples of the unstable evolution are displayed in Fig. 4. Panel (a) represents a simulation belonging to  $\gamma = 2$  showing the decaying (spreading out) evolution of the state. On the other hand, the evolution of a solution with  $\gamma = 4$ , in the VK-unstable region of the negative slope ( $\beta = 2$ ) is shown in panels (b) and (c). In this case the bullet, after an initial contraction which results in a collapse as is  $\beta$  large enough, follows a spreading out behavior (actually, the post-collapse evolution may be irrelevant, as the usual GPE may become invalid for a strongly collapsed state). At this point the bullet is stabilized in the  $(x, y)$  plane [see panel (b)] due to the action of the trapping potential, but is unstable in the axial direction, as shown in panel (c).

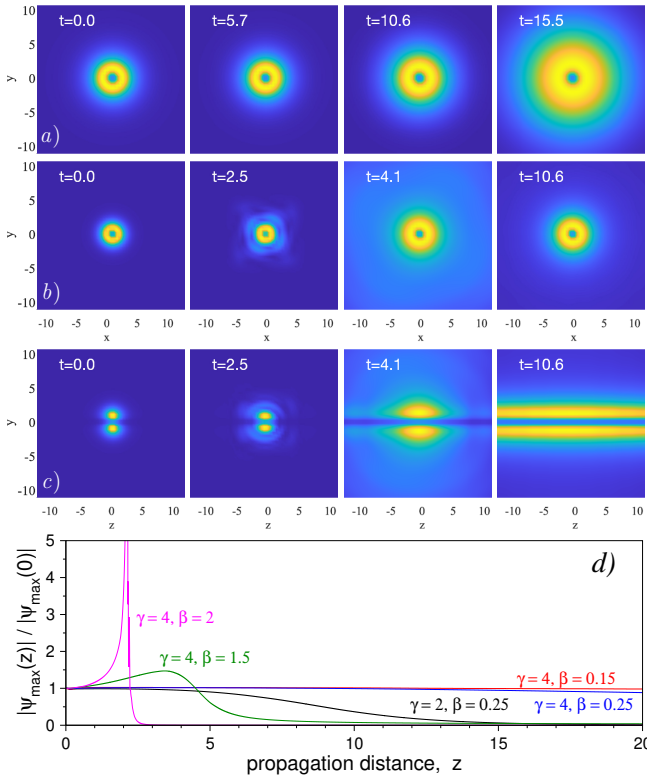


FIG. 4. The simulated perturbed evolution of two unstable solutions for a)  $\gamma = 2$ ,  $\beta = 0.25$  and b)  $\gamma = 4$ ,  $\beta = 2$ , plotted in the  $(x, y)$  plane. c) The same as in b), but in the  $(z, y)$  plane. d) The evolution of the field's amplitude (normalized to its value at  $t = 0$ ) for different solutions, as indicated (both stable, for  $\gamma = 4$ ,  $\beta = 0.15$  and  $\beta = 0.25$  and unstable for all other cases).

The evolution of the maximum amplitude for different solutions is shown in Fig. 4(d). In accordance to what is said above, the unstable solutions for  $\gamma = 4$ , *viz.* are destroyed by the initial contraction ( $\beta = 1.5$ ) or collapse ( $\beta = 2$ ). On the other hand, the instability of the mode with  $\gamma = 2$  and  $\beta = 0.25$  eventually does not lead to the

collapse, but to decay.

The systematic simulations demonstrate that the vortex solitons which belong to the VK-stable family, such as the one with  $\gamma = 4$  and  $\beta < 1.24$ , represented by the continuous green branch in Fig. 2, are indeed fully stable. Examples, plotted in Fig. 4(d) for  $\gamma = 4$  and  $\beta = 0.15$  and  $\beta = 0.25$ , corroborate the stability – at least, up to  $t = 200$  which, roughly speaking, corresponds to 20 characteristic diffraction times for these modes. The conclusion is that the potential should be sufficiently strong (approximately, with  $\gamma \gtrsim 3.1$ ) for maintaining the stability of the trapped vortex modes, and their propagation constant should not be too large.

Once stable vortex bullets are found, it is natural to test their robustness against mutual collisions in the unconfined direction ( $z$ ), cf. Ref.[29]. Simulations demonstrate in Fig. 5 that the repulsive head-on collision of two stable vortex bullets from Fig. 3, with opposite initial velocities, identical vorticities,  $\ell = 1$ , and the phase shift  $\pi$  (opposite signs) seems completely elastic, which is a typical outcome. In-phase collisions between the vortex bullets with identical signs are elastic too, leading to their mutual passage provided that the initial velocities are large enough (not shown here).

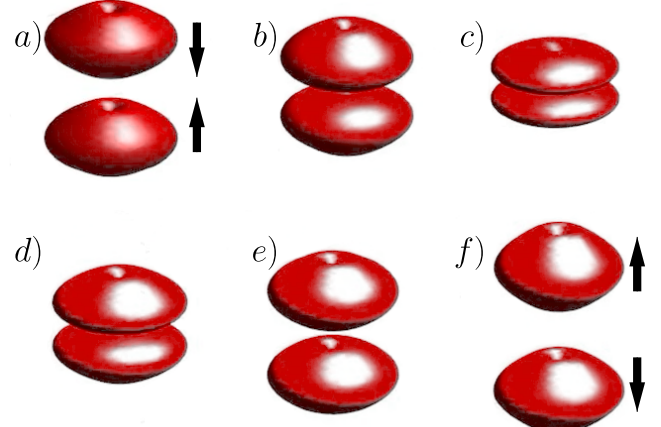


FIG. 5. The elastic head-on collision of two stable vortex bullets from Fig. 2 with opposite signs, which are set in motion along the  $z$  axis with opposite initial velocities. The collision leads to the elastic rebound of the solitons. The frames a) to f) correspond, respectively, to evolution times  $t = 0.0$ ,  $7.6$ ,  $15.2$ ,  $22.9$ ,  $30.5$ , and  $38.1$ .

*Conclusion.-* In this work we have studied the formation, stability, and propagation dynamics of bullets (3D solitons), carrying vorticity  $\ell = 1$ , in the 3D cubic self-focusing medium with the 2D axisymmetric trapping Gaussian potential. By means of the variational method and systematic numerical analysis, we have demonstrated, for the first time to our knowledge, the existence of stable vortex-carrying wavefunctions under experimentally accessible conditions, that may be realized in BEC and optics. The stability area for the vortex

bullets, and the dependence of their shape on the control parameters (the depth of the trapping potential and the bullet's norm) have been identified. Elastic collisions between the stable bullets moving in the unconfined direction have been demonstrated. Unstable bullets demonstrate either intrinsic collapse or spontaneous decay.

As an extension of the work it may be relevant to consider the bullets with multiple embedded vorticity, and also study collisions between ones with opposite vorticities. Also interesting is to extend the analysis for media with competing nonlinearities, which may be relevant for optics[30] and BEC[31] alike. Finally, a study of higher-charge vortices is interesting because, although it is known that they exhibit stronger azimuthal-modulation (splitting) instabilities, there is no universal topological argument that forces vortex bullets with

charge  $\ell > 1$  to be unstable. Several models with competing nonlinearities are known to support stable higher-charge vortices[32]. Exploring whether suitable trapping configurations may stabilize  $\ell > 1$  bullets in this setting is an interesting direction for further research.

Datasets generated for the figures are accesible (see Ref. [33]).

## ACKNOWLEDGEMENTS

This publication is part of the R&D&i project PID2023-146884NB-I00 funded by MCIN/AEI/10.13039/501100011033/. This work was also supported by grants ED431B 2021/22 and GPC-ED431B 2024/42 (Xunta de Galicia).

---

[1] B. A. Malomed, D. Mihalache, F. Wise, and L. Torner, Spatiotemporal optical solitons, *Journal of Optics B: Quantum and Semiclassical Optics* **7**, R53 (2005).

[2] Y. Silberberg, Collapse of optical pulses, *Optics letters* **15**, 1282 (1990).

[3] G. Fibich, *The Nonlinear Schrödinger Equation: Singular Solutions and Optical Collapse*, Applied Mathematical Sciences (Springer International Publishing, 2015).

[4] Y. S. Kivshar and G. P. Agrawal, *Optical solitons: from fibers to photonic crystals* (Academic press, 2003).

[5] V. M. Perez-Garcia, H. Michinel, and H. Herrero, Bose-einstein solitons in highly asymmetric traps, *Physical Review A* **57**, 3837 (1998).

[6] K. E. Strecker, G. B. Partridge, A. G. Truscott, and R. G. Hulet, Formation and propagation of matter-wave soliton trains, *Nature* **417**, 150 (2002).

[7] L. Khaykovich, F. Schreck, G. Ferrari, T. Bourdel, J. Cubizolles, L. D. Carr, Y. Castin, and C. Salomon, Formation of a matter-wave bright soliton, *Science* **296**, 1290 (2002).

[8] K. Shimizu and Y. H. Ichikawa, Automodulation of ion oscillation modes in plasma, *Journal of the Physical Society of Japan* **33**, 789 (1972).

[9] A. Paredes and H. Michinel, Interference of dark matter solitons and galactic offsets, *Physics of the Dark Universe* **12**, 50 (2016).

[10] N. N. Akhmediev, V. Korneev, and R. F. Nabiev, Modulation instability of the ground state of the nonlinear wave equation: optical machine gun, *Optics letters* **17**, 393 (1992).

[11] V. Bespalov and V. Taranov, Filamentary structure of light beams in nonlinear liquids, *Soviet Journal of Experimental and Theoretical Physics Letters* **3**, 307 (1966).

[12] C. Sulem and P.-L. Sulem, *The nonlinear Schrödinger equation: self-focusing and wave collapse*, Vol. 139 (Springer Science & Business Media, 2007).

[13] L. P. Pitaevskii, Vortex lines in an imperfect bose gas, *Sov. Phys. JETP* **13**, 451 (1961).

[14] F. Dalfovo, S. Giorgini, L. P. Pitaevskii, and S. Stringari, Theory of bose-einstein condensation in trapped gases, *Reviews of modern physics* **71**, 463 (1999).

[15] S.-S. Yu, C.-H. Chien, Y. Lai, and J. Wang, Spatiotemporal solitary pulses in graded-index materials with kerr nonlinearity, *Optics Communications* **119**, 167 (1995).

[16] D. Mihalache, D. Mazilu, F. Lederer, Y. V. Kartashov, L.-C. Crasovan, and L. Torner, Stable three-dimensional spatiotemporal solitons in a two-dimensional photonic lattice, *Phys. Rev. E* **70**, 055603 (2004).

[17] S. Raghavan and G. P. Agrawal, Spatiotemporal solitons in inhomogeneous nonlinear media, *Optics Communications* **180**, 377 (2000).

[18] J. F. Nye and M. V. Berry, Dislocations in wave trains, *Proc. Math. Phys. Eng. Sci.* **336**, 165 (1974).

[19] P. Coullet, L. Gil, and F. Rocca, Optical vortices, *Optics Communications* **73**, 403 (1989).

[20] V. Kruglov and R. Vlasov, Spiral self-trapping propagation of optical beams in media with cubic nonlinearity, *Physics Letters A* **111**, 401 (1985).

[21] C. Hang and G. Huang, Ultraslow helical optical bullets and their acceleration in magneto-optically controlled coherent atomic media, *Physical Review A—Atomic, Molecular, and Optical Physics* **87**, 053809 (2013).

[22] B. A. Malomed, *Multidimensional solitons* (AIP Publishing, Melville, New York, 2022).

[23] M. A. Porras, Upper bound to the orbital angular momentum carried by an ultrashort pulse, *Physical Review Letters* **122**, 123904 (2019).

[24] Z. Chen, M. Segev, D. W. Wilson, R. E. Muller, and P. D. Maker, Self-trapping of an optical vortex by use of the bulk photovoltaic effect, *Physical Review Letters* **78**, 2948 (1997).

[25] H. Zhang, T. Zhou, and C. Dai, Stabilization of higher-order vortex solitons by means of nonlocal nonlinearity, *Physical Review A* **105**, 013520 (2022).

[26] H. Leblond, B. A. Malomed, and D. Mihalache, Three-dimensional vortex solitons in quasi-two-dimensional lattices, *Phys. Rev. E* **76**, 026604 (2007).

[27] J. R. Salgueiro, D. Olivieri, and H. Michinel, Computation of linear and nonlinear stationary states of photonic structures using modern iterative solvers, *Optical and quantum electronics* **39**, 239 (2007).

- [28] N. G. Vakhitov and A. A. Kolokolov, Stationary solutions of the wave equation in a medium with nonlinearity saturation, *Radiophysics and Quantum Electronics* **16**, 783 (1973).
- [29] H. Leblond, B. A. Malomed, and D. Mihalache, Interactions of spatiotemporal solitons and vortices in fiber bundles, *Phys. Rev. A* **79**, 033841 (2009).
- [30] M. Quiroga-Teixeiro and H. Michinel, Stable azimuthal stationary state in quintic nonlinear optical media, *J. Opt. Soc. Am. B* **14**, 2004 (1997).
- [31] L. Dong, M. Fan, and B. A. Malomed, Three-dimensional vortex and multipole quantum droplets in a toroidal potential, *Chaos, Solitons & Fractals* **188**, 115499 (2024).
- [32] H. Michinel, J. R. Salgueiro, and M. J. Paz-Alonso, Square vortex solitons with a large angular momentum, *Phys. Rev. E* **70**, 066605 (2004).
- [33] Data for the paper "Guided vortex bullets" by Sanchez, Paredes, Michinel, Malomed and Salgueiro, 10.5281/zenodo.16672192 (2025).